

INFLUENCE OF STEEL FIBERS ON THE FATIGUE BEHAVIOR OF HIGH-PERFORMANCE CONCRETES UNDER CYCLIC LOADING

DAVID OV*, ROLF BREITENBÜCHER

Ruhr University Bochum, Department of Civil and Environmental Engineering, Institute for Building Materials, Universitätsstrasse 150, 44801 Bochum, Germany

* corresponding author: David.Ov@ruhr-uni-bochum.de

ABSTRACT.

Due to the advancement of high-performance concretes, the development of filigree constructions has been improved in the last decades. However, as the demand to create more filigree designs increases, the vulnerability to fatigue loads of such structures has also become a decisive factor. Various construction projects, such as wide-span bridges or wind turbines, are exposed to fatigue loads. Especially wind turbines are permanently subjected to wind and wave loads of several hundred million load cycles during their service life. At present, the fatigue behavior of high-performance concretes under cyclic loading is still unknown. In a worst-case scenario, the significantly lower ductility can lead to a sudden failure of the entire structure. In this case, the addition of steel fibers could be advantageous, as they significantly improve the ductility of concretes. However, it is still undetermined how the material fatigue is influenced by steel fibers. Hence, systematic investigations on the fatigue behavior of various high-strength concretes with steel fibers were conducted. Since the crack-bridging effect of fibers is relevant for tensile stresses, predominantly cyclic bending tests were performed on concrete beams with different steel fiber variations. To accomplish the investigations, a test setup has been developed which allows the simultaneous testing of a total of six specimens. Based on the predetermined static concrete strengths, the specimens were subjected to cyclic loads with a defined lower stress level and various upper stress levels. During these cyclic tests, the cycles-to-failure as well as the degradation within the microstructure were detected.

KEYWORDS: Cyclic loading, degradation, fatigue behavior, high strength concrete, steel fibers.

1. INTRODUCTION

With the increasing appearance of filigree designed structures, the necessity to investigate the fatigue behaviour of materials has become more significant in the past decades. Since the beginning of the 20th century, railway bridges with large spans have been constructed and the installation of e.g. offshore facilities followed. Many of those structures are exposed to fatigue stresses during their service life. Figure 1 provides an overview of various structures, which are subdivided in accordance with the numbers of load cycles during their lifetime [1]. Particularly wind turbines are subjected to wind loads of up to $N = 10^9$ load cycles, which endangers the foundation and tower construction as a result of material fatigue.

Due to the further development of high-performance concretes, it is possible to produce the tower construction of wind turbines in reinforced and prestressed concrete. However, an essential difference between high-performance concretes and normal concretes is their distinctly more brittle material behavior or significantly lower ductility. Considering the foundation of wind turbines, not only compressive forces but also tensile forces occur in the anchoring area. This may result in a sudden failure of the structure under permanent fatigue loading.

In this context, the addition of steel fibers could be advantageous, as they significantly improve the ductility and the post-cracking behavior by a crack-bridging effect in the concrete. However, the fatigue behavior of steel fiber-reinforced high-performance concrete (SFRHPC) under fatigue stress is still unexplored. In general, the overall test series described in the literature are limited to the fatigue behavior of normal steel fiber reinforced concrete under cyclic stress up to about $N = 10^6$ load cycles. For particularly high-performance concretes, the fatigue behavior has only been investigated occasionally so far, see e.g. [2] and [3]. An effective increase in the number of cycles-to-failure could clearly not be determined for SFRHPC, however, the concretes revealed a much more ductile elongation behavior, resulting in a prolonged phase of unstable crack growth [2]. As a result, these concretes showed better failure announcement behavior. In addition to the fiber content, the effectiveness of steel fibers is largely determined by the geometry and length of the fibers [4]. Therefore, the aim of this research study is to investigate the extent to which the addition of steel fibers influences the fatigue behavior of high-strength concretes.

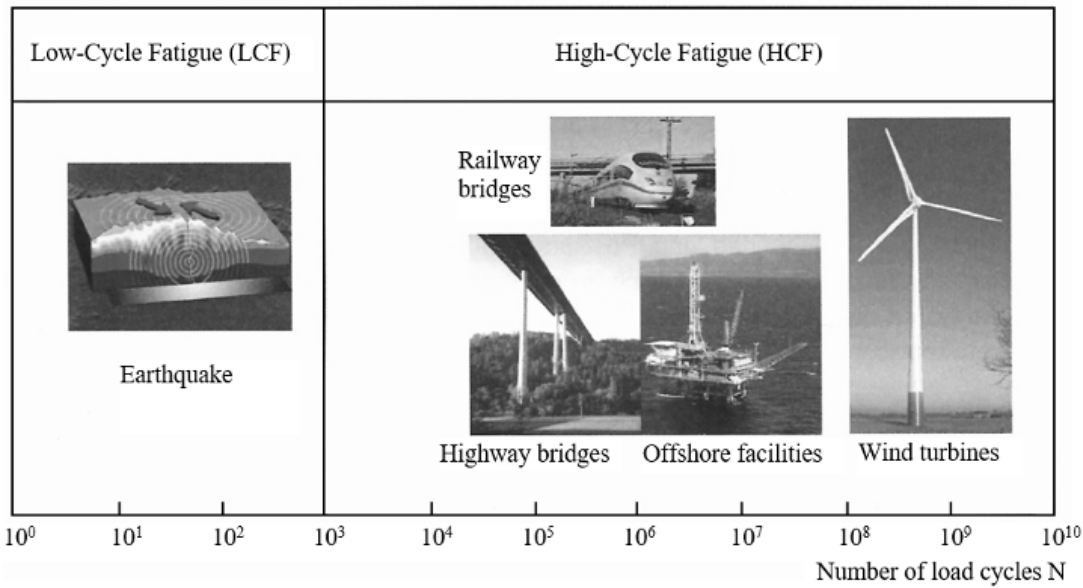


FIGURE 1. Number of load cycles of different cyclically stressed structures [1].

Components	C80	C120
Binder/Sand mixture	CEM I 52.5 R	CEM I 52.5 R
Aggregate 2/8 mm	Quartz Gravel	Quartz Gravel
Aggregate 8/16 mm	Limestone	Quartz Gravel
Superplasticizer	PCE based	PCE based
w/c-ratio (-)	0.47	0.35

TABLE 1. Concrete compositions of C80 and C120.

Steel fiber series	Shape	SLength l (mm)	Diameter d (mm)	Aspect ratio l/d (-)	Tensile strength f_t (MPa)
SF-A	straight	6	0.16	37.5	2,600
SF-B	straight	13	0.20	65.0	2,600
SF-C (Mix)	straight / hooked end	6 / 35	0.16 / 0.55	37.5 / 65.0	2,600 / 1,345

TABLE 2. Properties of the steel fiber series.

2. INVESTIGATION PROGRAM

2.1. CONCRETE COMPOSITIONS

As a basis for the following studies in this paper, particularly two high-performance concretes with compressive strengths of 80 MPa (C80) and 120 MPa (C120) were included in the experimental investigations. In addition to their high-strength properties, both concretes also have self-compacting properties, as they show a self-levelling and self-venting behavior after mixing. In principle, the composition of the two concretes were defined by an industrial partner in the form of a specified binder/sand mixture with a maximum aggregate size of 16 mm. The concrete compositions of C80 and C120 are listed in Table 1.

2.2. WORKABILITY WITH STEEL FIBERS

The first part of the experimental investigations was to examine the workability of the fresh concrete due to the addition of steel fibers and to define a suitable

maximum fiber dosage. For this purpose and in order to determine the influence of the steel fibers, different fiber variations (fiber geometry, tensile strength and aspect ratio) were specified. In this case, the selected variations are a high-strength micro-steel fiber with 6 mm length (SF-A series), an another high-strength micro-steel fiber with 13 mm length (SF-B series) and a fiber mix of 50 % micro-steel and 50 % macro-steel fibers (SF-C series). The characteristic properties of the different steel fiber series are listed in Table 2.

In order to assess the change in workability of the high-strength concretes with especially self-compacting properties, the slump flow and the t_{500} -time were determined according to EN 12350-8 [5]. During the examination, the mixtures of both concretes were not modified in general, e.g. the cement paste volume was not adjusted due to the addition of steel fibers. Only the superplasticizer content was adjusted to control the consistency and processing of

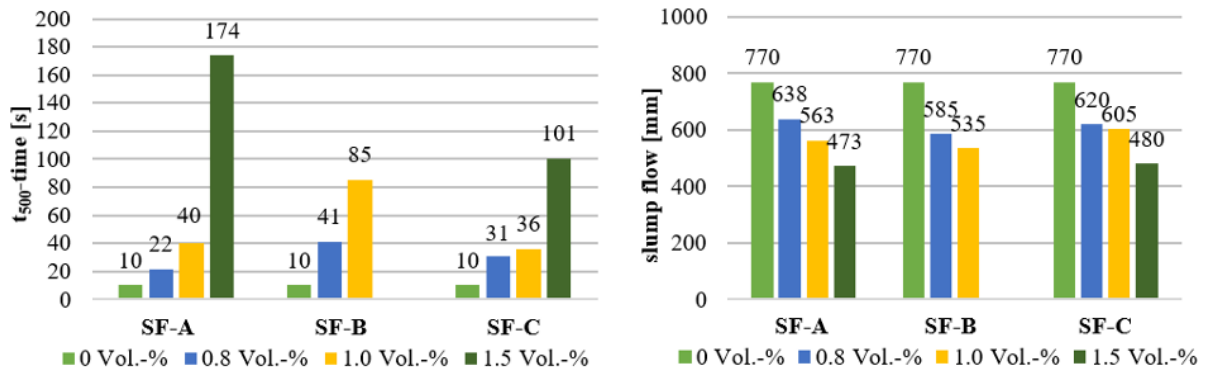


FIGURE 2. t_{500} -time (left) and slump flow (right) depending on the fiber variations and content.

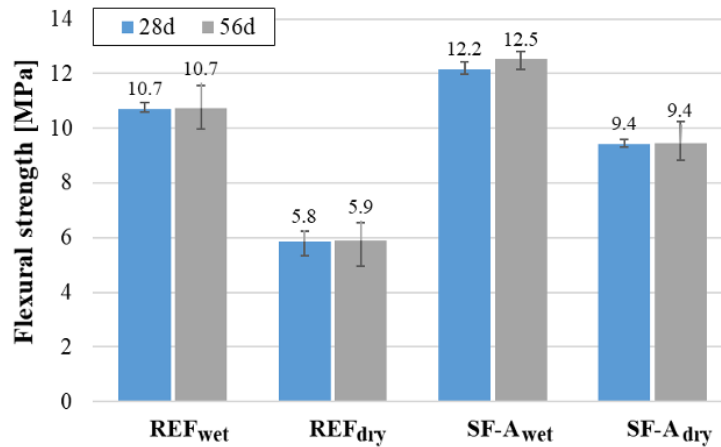


FIGURE 3. Flexural strength of C120 depending on the test age and preliminary storage.

the fresh concrete. The results of the t_{500} -time and slump flow tests, determined with the concrete C120 on different fiber dosages, are shown in Figure 2.

As can be seen from Figure 2, an affection of the fresh concrete properties can be detected with higher steel fiber content, since the tests results demonstrates a decreasing slump flow value and thus an increasing t_{500} -time. At a steel fiber content of 1.5 Vol.-%, occasional agglomerations could be observed in the fresh concrete regardless of the type of steel fibers. By slightly increasing the superplasticizer dosage, it was also possible to improve the slump flow of all mixtures with 1.0 Vol.-% fiber dosage to approx. 600-630 mm without any signs of segregation. Therefore, a maximum steel fiber content of 1.0 Vol.-% was defined for the following investigations.

2.3. FLEXURAL STRENGTH

Prior to the cyclic bending tests, it is necessary to examine the static strength of the concretes and thereby to be able to define the upcoming stress levels. Thus, the flexural strengths of concrete beams ($700 \times 150 \times 150 \text{mm}^3$) were determined according to the DAfStb German Guideline "Steel fibre reinforced concrete" [6] in a four-point flexural setup. In order to also take into account the influence of the pre-storage conditions, the test series were stored in a

preliminary study as follows: On the one hand, the specimens were stored under water according to EN 12390-2/A20 [7] until the time of testing and, on the other hand, stored in a dry environment (20°C , 65 % RH) after the 6th day of water. For this purpose, the fibre-free reference concrete (C120) and the steel fibre-modified concrete with SF-A (C120) were initially tested, see Figure 3.

At first glance, it can be stated that no significant increase in flexural strength due to post-curing was observed as a result of a later test period (56d). By adding the steel fibers (SF – A_{wet}), an increase in flexural strength of about 14 % could be achieved compared to the fiber-free samples (REF_{wet}). In the case of the dry-stored samples REF_{dry}, the flexural strength was measured to be about 46 % lower than REF_{wet} due to the resulting shrinkage stresses during dry storage. For REF_{dry} compared to SF – A_{wet}, however, only a reduction of the flexural strength of roughly 23 % was found, indicating a possible influence of the steel fibers on the shrinkage behavior or on the residual stresses.

In order to prevent the shrinkage stresses, the flexural strengths of the two concrete strength classes were subsequently investigated as dry stored specimens. Figure 4 shows the average flexural strength values of the concretes C80 (left) and C120 (right),

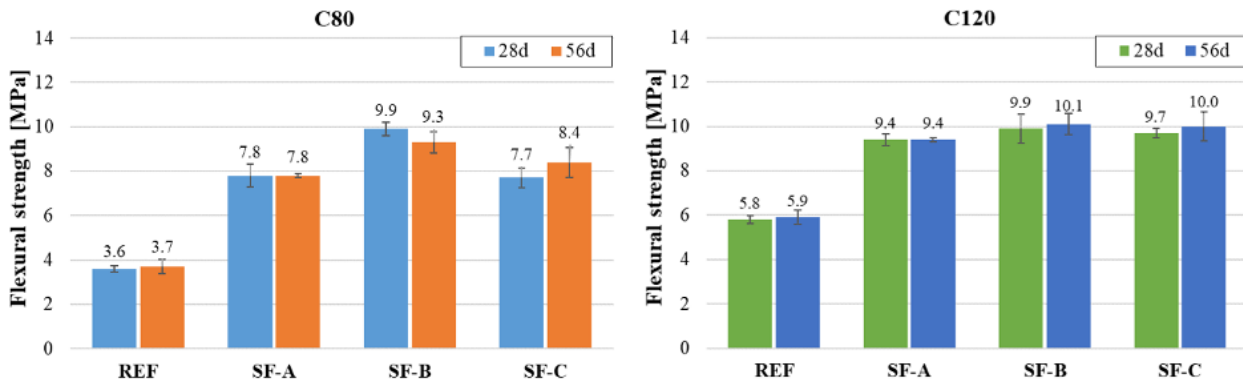


FIGURE 4. Average flexural strength of C120 and C80 depending on the different fiber variants.

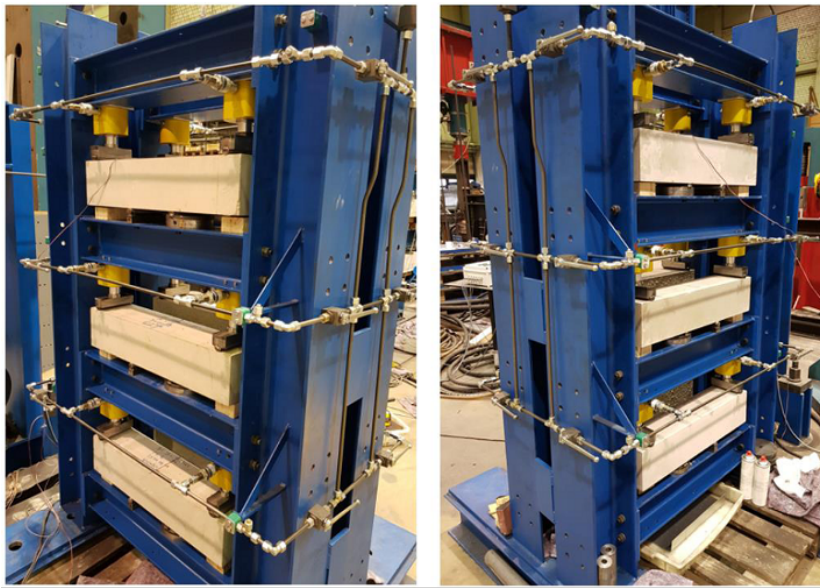


FIGURE 5. Test setup for the simultaneous loading of six specimens.

subdivided according to the specified fiber variations (REF, SF-A, SF-B and SF-C). The test specimens were also tested at concrete ages of 28d and 56d.

In terms of the observed test results, it can be stated that the development of the flexural strength also does not change significantly over time. Accordingly, it can be seen in each test series that the flexural strengths between 28d and 56d remain dominantly at the same level. The effect of adding fibers is again very noticeable from the results between REF and with steel fibers (SF-A, SF-B and SF-C).

2.4. CYCLIC BENDING TEST

2.4.1. TEST SETUP

In order to conduct the cyclic bending tests, an innovative test setup has been developed which enables the cyclic loading of six prismatic specimens ($700 \times 150 \times 150 \text{mm}^3$) at the same time and therefore substantially shortens the generally long procedure of fatigue tests. In principle, the test setup is hydraulically operated and the frame is designed in a way that allows three specimens to be placed on each side (see Figure 5). A main hydraulic cylinder leads the pres-

sure into the system, where it is distributed to each of the six individual test positions. This method ensures a reliable reproducibility, as all six specimens are subjected to the same pressure and force simultaneously.

At each individual test positions there are two smaller modified hydraulic cylinders, which can transfer a pre-defined pressure of up to 200 bar into the specimens with a frequency of 5 Hz (see Figure 6, left). All concrete beams were subjected to the cyclic stresses at a minimum age of 56 days and in a four-point-flexural setup, so that the maximum bending tensile stress is located on the upper side of the beam. Accordingly, when the concrete reaches the number of cycles-to-failure, the cracking occurs on the upper side of the specimen (see Figure 6, right).

2.5. DEGRADATION

In addition to the determination of the number of cycles-to-failure, the stiffness development of the concretes was also monitored during the fatigue tests. Especially by examining the stiffness, a progressive degradation of the test specimens can be visualized

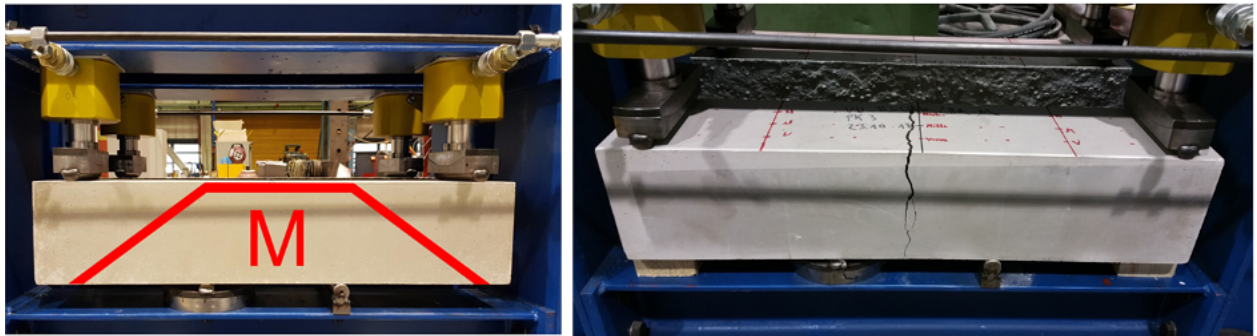


FIGURE 6. Display of max. bending stress in the test specimen (left) and an example of crack (right).

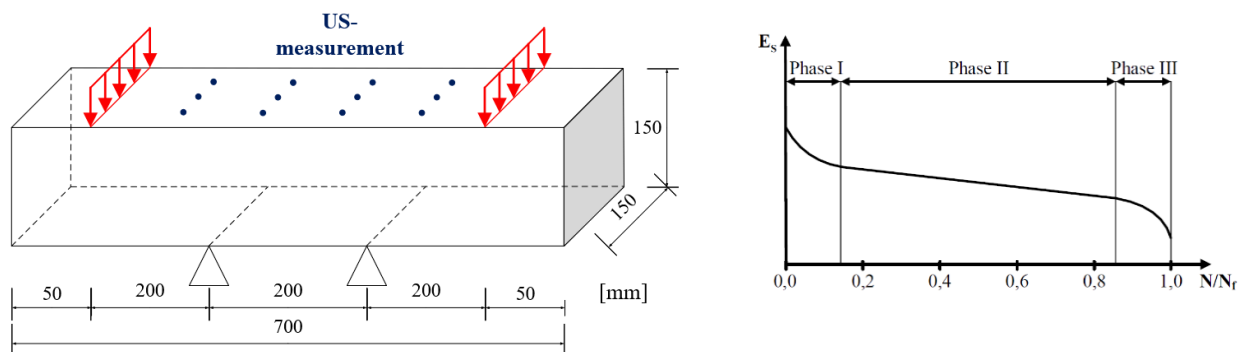


FIGURE 7. Schematic test arrangement for US (left) and course of stiffness development (right [8]).

[9]. This degradation within the concrete structure caused by cyclic bending stresses was measured after specified numbers of load cycles by means of comparative ultrasonic runtime measurements (longitudinal waves) in the area of maximum bending stresses (Figure 7, left). For this purpose, a suitable ultrasonic measuring device was used.

Based on the ultrasonic runtime measurements, the dynamic modulus of elasticity can be determined. A continuous reduction in the relative dynamic E-modulus over the loading periods indicates an increasing number of microcracks as well as other microstructural changes in the concrete structure [9]. If the determined stiffnesses is plotted against the number of load cycles or against the related number of load cycles, an S-shaped curve is formed that can basically be divided into three phases (see Figure 7, right).

2.5.1. RESULTS

For the fatigue tests under cyclic bending stress, preliminary studies on the influence of the pre-storage (between wet and dry) were also required and thereby conducted. In that case, three test specimens without steel fibers (REF) as well as three test specimens with steel fibers (SF-A) were again included and tested with up to $N = 10^7$ load cycles at a frequency of 5 Hz. The setting of the upper and lower stresses based on the results of the static flexural strength tests and was determined as follows:

- upper stress $\sigma_o = 0.60 \cdot f_{ct, fl}$
- lower stress $\sigma_u = 0.30 \cdot f_{ct, fl}$

Figure 8 shows the courses of the rel. dynamic E-modulus for the specimens without steel fibers (REF) and with steel fibers (SF-A) of concrete C120.

Following the developments of the rel. dyn. E-modulus, a significant degradation already occurs in the early load cycles. As expected, the REF_{wet} specimens already failed after roughly 300,000 load cycles due to the shrinkage stresses superimposed by cyclic loading. However, a failure of the SF-A specimens did not occur even after 10 million load cycles. But a continuous decrease in the rel. dynamic E-modulus was notable. In a first phase up to about 500,000 load cycles, a relatively steep decrease in the rel. dynamic E-modulus is caused by the initiation of microcracks. This is followed by a flatter decline of the rel. dynamic E-modulus. When comparing the wet and dry stored test series, significant differences can be observed. While the rel. dyn. E-modulus of the wet-stored SF-A test specimens is around 76.5 % after 10 million load cycles, the rel. dyn. E-modulus of the dry-stored SF-A test specimens is around 89.7 %. One of the reasons for the early failure of the REF_{wet} test specimens is the drying out and the associated additional shrinkage stresses as these series had been stored in water until the test day.

Under consideration of the results of the preliminary studies, the following test series are stored solely in a dry environment in order to reduce the dry-

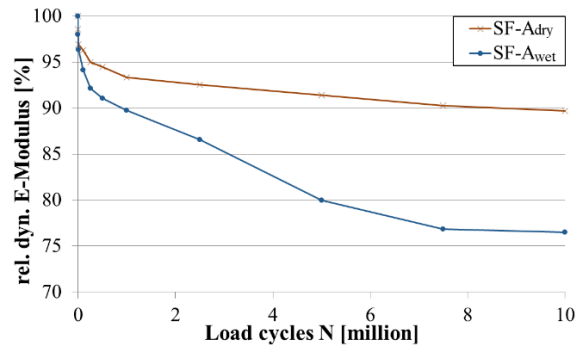
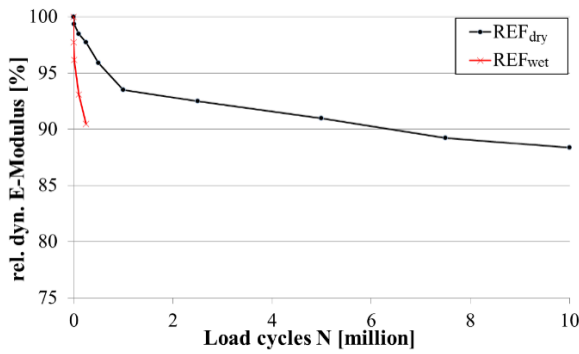


FIGURE 8. Decrease of the rel. dyn. E-modulus of REF (left) and SF-A (right).

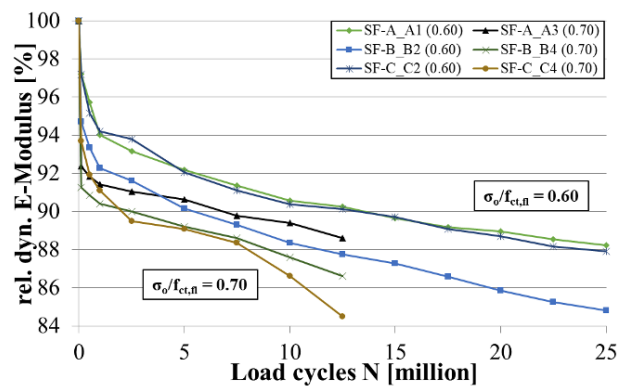
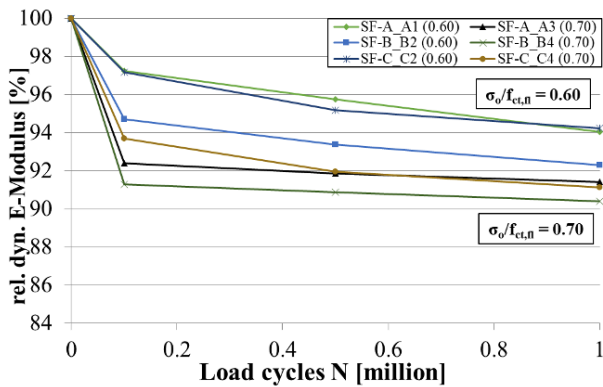


FIGURE 9. Decrease of the rel. dyn. E-modulus of SF-A, SF-B and SF-C at various upper stresses.

ing effects (shrinkage stresses). Subsequently, the concrete C120 was further examined (up to $N = 2.5 \cdot 10^7$), taken into account the influence of different fiber variations and additionally various stresses $\sigma_o = 0.60, 0.70$ and $\sigma_u = 0.30$ (Figure 9).

The results with an upper load of 0.70 are interim results, which are currently recorded up to 12.5 million load cycles. According to the diagrams it can be observed, that the higher the load stress, the greater the drop in the relative dynamic modulus of elasticity becomes. After 100,000 load cycles, a drop to 95.3 % (SF-A), 94.7 % (SF-B) and 97.2 % (SF-C) was observed at a load level of $\sigma_o/f_{ct,fl} = 0.60$, whereas a significantly higher drop to approx. 92.4 % (SF-A), 91.3 % (SF-B) and 93.7 % (SF-C) was already noticed at $\sigma_o/f_{ct,fl} = 0.70$. All test samples have passed through up to 12.5 and 25 million load cycles without failure. Regardless of the load level, the loss of stiffness is particularly evident within the first few load cycles. Furthermore, it can be seen that the relative dynamic E-modulus of all test specimens decreases further with increasing number of load cycles, as expected. The falling curves show the typical S-shaped course of fatigue tests.

3. CONCLUSION

In order to study the influence of steel fibers on the fatigue behavior of high-performance concretes, predominantly cyclic bending tests on concrete beams

($700 \times 150 \times 150 \text{mm}^3$) with different steel fiber variations (SF-A, SF-B and SF-C) were conducted. During these cyclic tests (up to $N = 2.5 \cdot 10^7$), the cycles-to-failure as well as the degradation within the microstructure were monitored. The presented test results reveal a significant influence of the cyclic bending tests ($N = 10^7$) on the effectiveness of the steel fiber (SF-A) when compared with a fiber-free concrete (REF). As the the number of load cycles increased, a steady drop in the dynamic E-modulus could be detected without the steel fiber-modified test specimens failing in contrast to the fiber-free test specimens (REF_{wet} failed after 300,000 load cycles). The steel fiber modified test samples were all able to pass through up to 12.5 and 25 million load cycles without any failures. For the following studies, further experimental investigations on series with more fiber variants are planned. Moreover, microscopic examinations are planned to examine the microstructure in case of degradation. Additionally, a comparison of the fatigue behavior between high-strength and normal-strength steel fiber reinforced concretes is intended.

ACKNOWLEDGEMENTS

The research presented in this paper is part of the joint project WinConFat (project no. 0324016D) funded by the German Federal Ministry for Economic Affairs and Energy (BMWi). The authors are grateful for their financial support.

REFERENCES

- [1] J. Hegger, T. Roggendorf, C. Goralski, et al. Ermüdungsverhalten von Beton unter zyklischer Beanspruchung aus dem Betrieb von Windkraftanlagen. *Abschlussbericht, Fraunhofer IRB-Verlag Stuttgart* **3305**, 2014.
- [2] L. Lohaus, N. Oneschkow, K. Elsmeier, et al. Ermüdungsverhalten von Hochleistungsbetonen in Windenergieanlagen. *Bautechnik* **89**(8):533-41, 2012. <https://doi.org/10.1002/bate.201200024>.
- [3] E. Fehling, M. Schmidt, T. Teichmann, et al. Entwicklung, Dauerhaftigkeit und Berechnung Ultrahochfester Betone (UHPC). Schriftenreihe Baustoffe und Massivbau - Structural Materials and Engineering Series 3, *Kassel University Press*, 2005.
- [4] P. B. Cachim, J. A. Figueiras, P. A. A. Pereira. Fatigue behavior of fiber-reinforced concrete in compression. *Cement and Concrete Composites* **24**(2):211-7, 2002. [https://doi.org/10.1016/s0958-9465\(01\)00019-1](https://doi.org/10.1016/s0958-9465(01)00019-1).
- [5] EN 12350-8 2010. Testing fresh concrete - Part 8: Self-compacting concrete - Slump-flow test, 2010.
- [6] DAfStb. DAfStb Guidline - Steel fibre reinforced concrete, *Deutscher Ausschuss für Stahlbeton e. V.*, 2012.
- [7] EN 12390-2/A20 2015. Testing hardened concrete - Part 2: Making and curing specimens for strength tests; Amendment A20, 2015.
- [8] N. Oneschkow. Analyse des Ermüdungsverhaltens von Beton anhand der Dehnungsentwicklung, Hannover: Leibniz University Hannover, Ph.D. Thesis, 2014.
- [9] R. Przondziono, J. J. Timothy, M. Nguyen, et al. Vorschädigungen in Beton infolge zyklischer Beanspruchungen und deren Auswirkung auf Transportprozesse im Hinblick auf eine schädigende AKR. *Beton- und Stahlbetonbau* **110**(1):3-12, 2015. <https://doi.org/10.1002/best.201400095>.